Nahrain University, College of Engineering Journal (NUCEJ) Vol.16 No.2, 2014 pp.238-259

Modeling Design of Solar Heating System for Absorption Refrigeration System with Partial Loads & Studying the Collectors arrangements

Mohammed Hadi Ali
University of Mustansiriya

Abstract:

This paper presents a modeling design for a solar heating system to be used as a driven - powered thermal energy to a single – stage absorption cooling system using Lithium Bromide solution, by using flat – plate collectors, storage tank, auxiliary heater and 3 – way valves. The study also goes into partial load control by flowrate variation through the generator section and to study the effects of series and parallel collector's arrangement arrays on the solar heating system performance.

The study is focused to evaluate the performance of the solar heating system throughout the summer season. The effects on performance have been explored for various design variables and operation conditions.

In this paper, it was reached to a general formula for a collector outlet temperature arranged in series and compared to a parallel arrangement.

The performance calculations indicate that:

- There is no significant difference in storage tank temperature for both parallel and series arrangements.
- The collector's outlet temperature wasn't greatly affected by the storage tank capacity (size).
- The storage tank temperature increases with partial load
- Percent increases, i.e. as the thermal load decreases.

Nomenclature:

A_c = Collector aperture area (m^2)
C_{pg} = Specific heat for the Water or water / glycol mixture in collector (W. s / kg. ^oC)
C_{pw} = Specific heat for the Water (W. s / kg. ^oC) = 4184
F_R (□□) = Solar Absorptivity coefficient is a number between [0 and 1] (Dimensionless)
$F_R U_L$ = Thermal Loss coefficient ($W/m^2 .^oC$)
I = The Average monthly Insolation (W/m^2)
I_{noon} = The peak noontime Solar radiation (W / m^2)
I_t = The Global solar radiation (W/m^2)
K_1 = Constant (Dimensionless)
K_2 = Constant ($m^2 . ^oC / W$)
K_3 = Constant (Dimensionless)
K_4 = constant (1 / s) = constant * 3600 (1 / hour).
K_5 = constant (1 / s) = constant * 3600 (1 / hour).
K_6 = $K_4 + K_5$ (1 / s) = constant * 3600 (1 / hour).
K_7 = Constant (1 / s) = Constant * 3600 (1 / hour)
K_8 = Constant ($m^2 . ^oC / W. s$) = Constant * 3600 ($m^2 . ^oC / W. hour$)
K_9 = Constant (1 / s) = Constant * 3600 (1 / hour)
K_{10} = Constant (1 / s) = Constant * 3600 (1 / hour)

M_{st} = Mass of the water in storage tank (kg)
m_{co-n} = Mass flow rate through the collectors in series (kg/s) = n . m_{co}
m_{co-t} = Total mass flow rate through the collectors (kg/s)
m_s = Mass flow rate through the storage tank (kg/s)
q_L = The heat losses from the storage tank & heat exchanger losses (W)
Q_{load} = Q_G (W), [equations (11 or 12)]
Q_{aux} = the heat added by the auxiliary heater (W), equation (14)
T_a = The ambient temp. (^oC)
T_{ci} = Collector inlet water temp. (^oC)
T_{co} = Collector outlet temp. of the Water or water / glycol mixture (^oC)
T_{co-n} = Collectors outlet temp. of the fluid medium (^oC)
T_{mix-1} = City Water or feed water temp. to the storage tank (^oC)
T_{st} = Storage tank water temp. (^oC)
t = Time (Hour)
$t_{sunrise}$ = The Sunrise time (Hour)
t_{sunset} = The Sunset time (Hour)
ΔT = The driving force temperature difference (^oC) [ref. 13]
□ = The collector efficiency
% Solar Availability = the percent of daily insolation available.

Introduction

The standard of living is closely linked to the energy consumption, a simple calculation shows the dramatic challenges facing the energy sector in the coming (100) years [ref. 1].
The world demand of energy for Air Conditioning is continually increasing. As traditional cooling units are electrically powered, peak demands of electrical power in summer increases and tend to reach the capacity limit in some countries [ref. 2].
In some ways, solar energy is better suited to space cooling and refrigeration than to space heating [3]. The seasonal variation of solar energy is well-suited to the space-cooling than heating requirements of buildings. Because the warmest seasons of the year correspond to periods of high insolation (incident solar radiation), thus solar energy is most available when there is no heat load but instead comfort cooling is most needed. Moreover, the efficiency of solar collectors increases with increasing insolation and increasing ambient temperature. In summer, the amount of energy delivered per unit area of collector can be larger than that in winter as a result of lower sun altitude angle, and may be cloudy, foggy and windy day.The traditional refrigeration & air conditioning system has not become popular due to the unfavorable economics and using more conventional means such as fossil fuels which has the greenhouse effect to environment. The most widely used methods applied to solar cooling and
air conditioning are vapor compression cycles, absorption-cooling cycles, and desiccant cooling [ref. 3].
Absorption air conditioning is a heat operated cycle [4], and it is compatible with solar energy because a large fraction of the energy required is thermal energy at temperatures that solar collectors can easily provide [3]. The LiBr – H_2O (Lithium Bromide – Water) system operates at a generator temperature in the range of [70 – 95 °C] with water used as a coolant in the absorber and condenser and has (COP) of about [0.7] and higher than NH_3 – H_2O (Ammonia – Water) system [ref. 6].

A simple solar absorption LiBr – H_2O system is shown in figure (1), and it is simply consists of two systems (circuits) as well a control panel, those are:

- Solar Heating system as a heat driven source for Absorption Refrigeration system (ARS).
- The LiBr – H_2O Absorption Refrigeration System (single stage) uses LiBr (Lithium Bromide) as absorbent and water as refrigerant and for application above (0 ℃).
- A control panel is to regulate the Flowrate to the generator of (ARS) at partial load and to control the storage tank temperature as it exceeds the reference set temperature to generator.

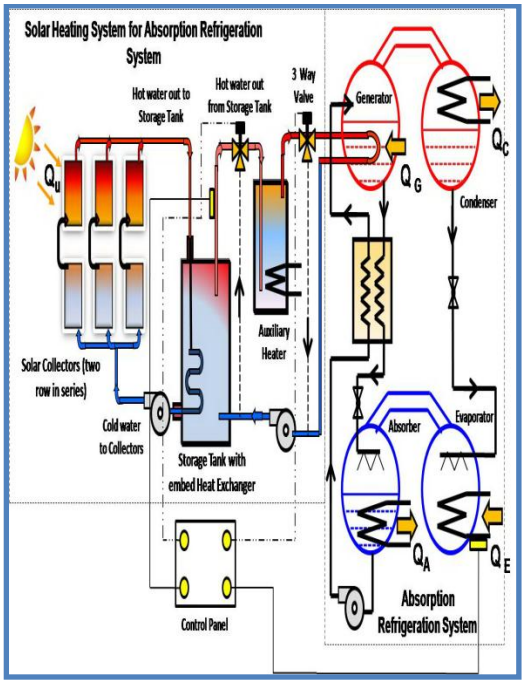

Fig. (1): The basic arrangement of a solar driven absorption refrigeration cycle.

The Objective of the Research:

The objective of this paper is to set a modeling design for improving solar thermal heating system for supplying a driven heat to an Absorption Refrigeration System (ARS), where the generator section for (ARS) is the only portion that is exposed to the solar heating system [ref. 7]. Most the concerned studies about the solar thermal absorption cooling system (STACS) focused on improving the performance of the absorption cooling systems rather than solar systems, because the solar system is a complex dynamic system and it is difficult to predict the annual saving energy, so, if experiments were used to study the effect of each parameter on the overall system performance would normally requires several cooling seasons to establish a conclusion [ref. 4 & 5].

Solar Absorption Refrigeration system – basic description:

A simple schematic drawing showing the most components, temperature, flow rates and flow direction of the solar absorption refrigeration– single effect LiBr – H_2O system are shown in figures (1 & 2). The working fluid in absorption refrigeration LiBr – H_2O system is a binary solution consisting of water as refrigerant and LiBr as absorbent.

Heat supplied by the solar heating system into the generator section is added to a solution of (LiBr-H_2O). This heat causes the refrigerant (water), to be boiled out of the solution in a distillation process. The water vapor that results passes into the condenser section where a cooling medium is used to condense the vapor back to a liquid state. The water then flows down to the evaporator section where it passes over tubes containing the fluid to be cooled. By maintaining a very low pressure in the absorber-evaporator shell, the water boils at a very low temperature. This boiling causes the water to absorb heat from the medium to be cooled, thus, lowering its temperature. Evaporated

water then passes into the absorber section where it is mixed with (LiBr-H_2O) solution that is very low in water content. This strong solution (in LiBr) tends to absorb the vapor from the evaporator section to form a weaker solution. This is the absorption process that gives the cycle its name. The weak solution is then pumped to the generator section to repeat the cycle.

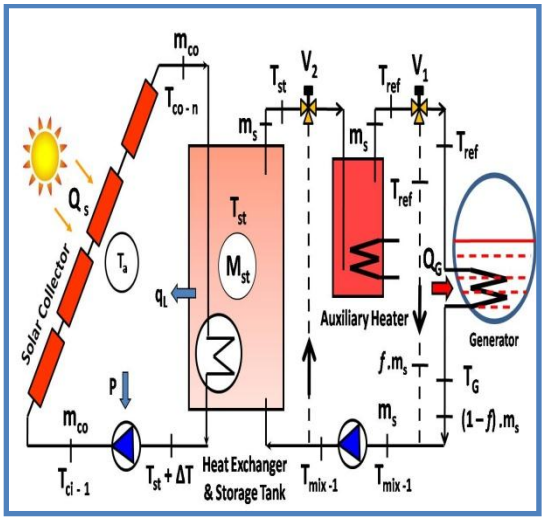

Fig. (2): Schematic diagram of Solar Absorption Refrigeration System (exposing generator section only)

On the other hand, the solar heating system consists of the solar collectors' arrays (parallel & series arrangement) in which the sun's energy is gained and transferred to circulating fluid, then, the heat is accumulated in the storage tank for direct or later use. The auxiliary heater is used to elevate the fluid temperature to specified or reference temperature (T_{ref}). The hot water is then supplied to the generator to boil off water vapor from a solution of LiBr and water.

A control panel (system) as well is used to regulate the flowrate to bypass through 3- way valve (V_1) for capacity control (partial load) of the (ARS), and to control the outlet temperature of the storage tank not to exceed (T_{ref}) or when it is less than fluid entering temperature to the storage tank (T_{mix-1}) by letting the fluid medium passing through 3-way valve (V_2).

The Theoretical Analysis of the Solar Heating System:

The solar heating system is modeled by treating each of the major components, which are solar collectors, storage tank, auxiliary heater, 3-way valves and the generator of the (ARS) by taking the energy and mass balance across each components.

We have assumed that only the input and output parameters are counted. This is the principle of a lumped parameter model (LPM) [ref. 7], which states that the volume or mass under consideration is perfectly mixed, all phases inside this volume will have the same property as that at the output. To study and analyze this case figure (2) above is applied to represent a simplified schematic for solar model (System Configuration).

The Heat Balance for the Solar Collectors:

The heat supplied by the solar heating system to the (ARS) should be at high temperature in the range of (70 – 95 ℃), in order to achieve this temperature an analysis of collectors arrangement in series is studied below. Thus, n – collectors of the same type are connected in series, and the flow through them(m_{co-n}) which is (n) times that of the single panel flow rate (m_{co}) [ref. 8] is required to obtain temperature in that range.

Referring to figure (3), the useful energy (Q_s) in watts gains from the sun as an incident solar radiation (I_t) on 1st collector will be absorbed by the

collector flow rate (m_{co-n}), the heat balance equation is:

$$Q_s = m_{co-n} . C_{pg} . (T_{co} - T_{ci}) \quad \ldots\ldots (1)$$

But (Q_s) is also found within acceptable accuracy limits for the Glazed Flat Plates & Evacuated Tube Collector [ref. 12] in terms of weather conditions (I_t & T_a) and inlet temperature (T_{ci}) to be equal to:

$$Q_s = A_c . [F_R (\tau\alpha) . I_t - F_R U_L . (T_{ci} - T_a) \quad \ldots\ldots (2)$$

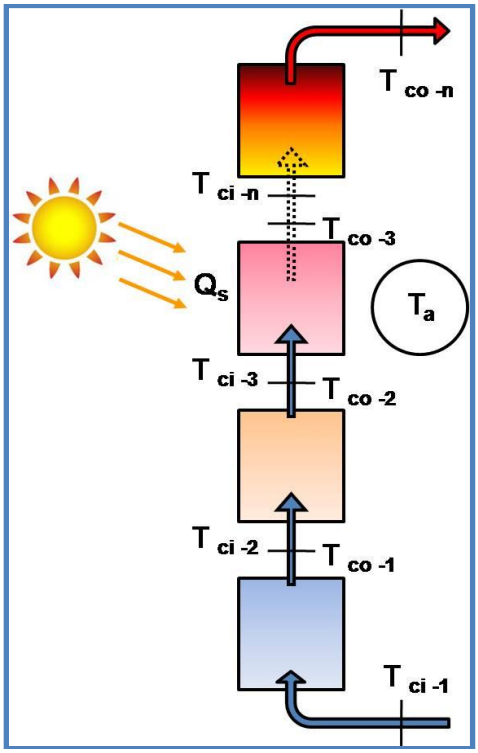

Fig. (3): Schematic drawing for Collectors in series.

Solving for (T_{co}) from equations (1 & 2), we will obtain that:

$$T_{co} = T_{ci} + \frac{A_c}{m_{co} . C_{pg}} [F_R (\tau\alpha) . I_t - F_R U_L (T_{ci} - T_a)] \quad \ldots\ldots (3)$$

By letting, [$a = \frac{A_c}{m_{co} . C_{pg}}$, $b = F_R (\tau\alpha)$, and $e = F_R U_L$], the above equation becomes:

$$T_{co} = (1 - ae) . T_{ci} + a . [b . I_t + e . T_a]$$

$$T_{co} = z . T_{ci} + a . w \quad \ldots\ldots (4)$$

Where:

$$z = 1 - ae , \quad \text{and} \quad w = [b . I_t + e . T_a]$$

Equation (3) can now be used for [n] collectors in series, as shown below:

For the 1st collector:

$$T_{co-1} = z . T_{ci-1} + a . w \quad \ldots\ldots (5)$$

For the 2nd collector: the inlet temperature for the 2nd collector (T_{co-2}) is the outlet temperature for the 1st collector (T_{co-1}), i. e, [$T_{co-1} = T_{ci-2}$], so, if we solve for (T_{co-2}) by using eq. (3) and substituting for (T_{co-1}) from eq. (5), that will yield to:

$$T_{co-2} = T_{co-1} + \frac{A_c}{m_{co-n} . C_{pg}} [F_R (\tau\alpha) . I_t - F_R U_L (T_{co-1} - T_a)]$$

$$T_{co-2} = (1 - ae) . T_{co-1} + a [b . I_t + e . T_a]$$

$$T_{co-2} = z . (z . T_{ci-1} + a . w) + a . w$$

Or, it can be write in term of (a, w and z) to become:

$$T_{co-2} = z^2 . T_{ci-1} + z . a . w + a . w \quad \ldots\ldots (6)$$

For the 3rd collector: solving for (T_{co-3}) to get a new equation:

$$T_{co-3} = z^3 . T_{ci-1} + + z^2 . a . w + z . a . w + a . w$$

$$T_{co-3} = z^3 . T_{ci-1} + (z^2 + z + 1) . a . w \quad \ldots\ldots (7)$$

In the same manner for further collectors in series, we will reach to a general equation for the outlet temperature (T_{co-n}) for [n – collectors] in series, which is as follows:

$$T_{co-n} = z^n . T_{ci-1} + (z^{n-1} + z^{n-2} + \cdots + 1) . a . w$$

$$T_{co-n} = z^n . T_{ci-1} + \sum_{1}^{n} z^{n-1} . a . w \quad \ldots\ldots (8)$$

Substituting for (w) in eq. (8), the general equation becomes:

$$T_{co-n} = z^n . T_{ci-1} + \sum_{1}^{n} z^{n-1} . a . [\, b . I_t + e . T_a \,]$$

$$T_{co-n} = z^n . T_{ci-1} + \sum_{1}^{n} z^{n-1} . a . b . I_t + \sum_{1}^{n} z^{n-1} a . e . T_a$$

$$T_{co-n} = K_1 . T_{ci-1} + K_2 . I_t + K_3 . T_a \quad \ldots\ldots (9)$$

Where:

$$K_1 = z^n = \left(1 - \frac{A_c . F_R U_L}{m_{co-n} . C_{pg}}\right)^n , \quad K_2 = \sum_{1}^{n} \left(1 - \frac{A_c . F_R U_L}{m_{co-n} . C_{pg}}\right)^{n-1} * \frac{A_c . F_R (\tau \alpha)}{m_{co-n} . C_{pg}} ,$$

$$K_3 = \sum_{1}^{n} \left(1 - \frac{A_c . F_R U_L}{m_{co-n} . C_{pg}}\right)^{n-1} * \frac{A_c . F_R U_L}{m_{co-n} . C_{pg}}$$

The Heat Balance for Storage Tank:

The water inside the storage tank is assumed to be well mixed and not stratified during heating up process in any way. The model loop is shown in figure (**4**) and the firm equation will be derived below as follows using simple energy balance along with mass flow and heat capacity for each stream and components. The heat balance equation for the storage tank is:

$$-M_{st} . C_{pw} . \frac{dT_{st}}{dt} = - m_{co-t} . C_{pg} . [\, T_{co} - (T_{st} + \Delta T)] + m_s . C_{pw} . (T_{st} - T_{mix-1}) + q_L$$

In this model, we ignore the effect of the tank size and assume all energy extracted by the solar panels is useful, and simply multiplied by the heat exchanger efficiency ($\boldsymbol{\eta}$), that means we let the heat loss (q_L) as a fraction of the of the useful energy of the built – in heat exchanger { $Q = m_{co-n} . C_{pg} . \boldsymbol{\eta} [\, T_{co} - (T_{st} + \Delta T)]$}, then the above equation becomes:

$$-M_{st} . C_{pw} . \frac{dT_{st}}{dt} = - m_{co-t} . C_{pg} . \eta . [\, T_{co-n} - (T_{st} + \Delta T)] + m_s . C_{pw} . (T_{st} - T_{mix-1})$$

Simplifying and re-arranging the above equation, it yields to:

$$\frac{dT_{st}}{dt} + K_6 . T_{st} = K_4 . T_{co-n} + K_5 . T_{mix-1} - K_4 . \Delta T \quad \ldots\ldots (10)$$

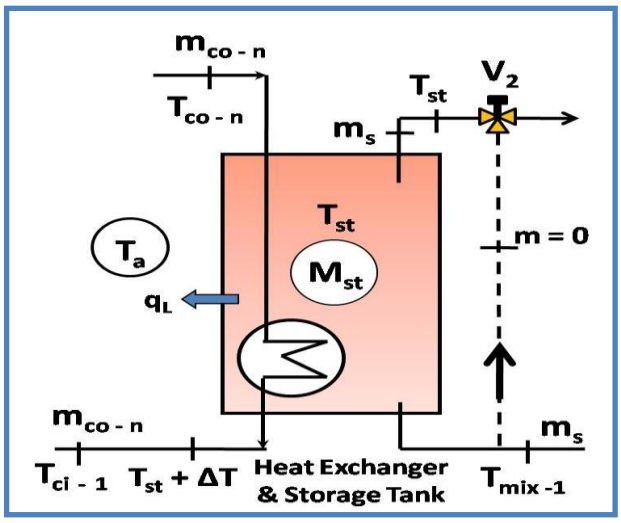

Figure (4): Schematic diagram of storage tank with built in heat exchanger

.

Where:

$$K_4 = \frac{m_{co-t}\, C_{pg}.\, \eta}{M_{st}\, .\, C_{pw}}, \qquad K_5 = \frac{m_s}{M_{st}}, \qquad K_6 = K_4 + K_5$$

The Heat & Mass Balance for the Generator section of (ARS):

In the generator section of the (ARS), the hot water comes from the (AH) will flow directly into the generator when the system is worked at its full capacity [fig. (5a)]. At partial load [fig. (5b)], the flowrate of the hot water to the generator is variable in order to keep the fluid outlet temperature constant [ref. 2, 14]. This is done by passing a fraction of flowrate ($f_1.\, m_s$) through 3 – way valve (V_1), as one method of capacity control. So, we have 2 cases to study, those are:

$$f_1 = \begin{cases} 0, & \text{at full capacity} \\ > 0, & \text{at partial capacity} \end{cases}$$

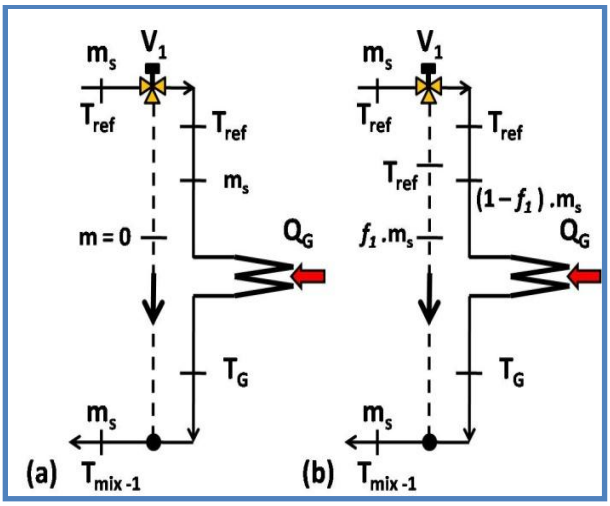

Figure (5): Schematic diagram of the Generator section of (ARS) & 3 – way valve (V_1).

The 1st case, [fig. (5a)] the heat added into the generator section (Q_G) of (ARS) by the solar system will be equal to:

$$Q_G = m_s.\, C_{pw}.\, (T_{ref} - T_G) \qquad \ldots\ldots (11)$$

And, the 2nd case, the heat added into the generator section of (ARS) [fig. (5b)], to maintain the temperature (T_G) constant, it will become:

$$Q_G = (1 - f_1).\, m_s.\, C_{pw}.\, (T_{ref} - T_G) \qquad \ldots\ldots (12)$$

$$T_{mix-1} = f_1.\, T_{ref} + (1 - f_1).\, T_G \qquad \ldots\ldots (13)$$

The Heat & Mass Balance for the Auxiliary Heater:

As mentioned previously, the auxiliary heater (AH) is used to elevate the fluid medium temperature coming out from the storage tank to reference temperature which is not less than the minimum allowable temperature to the generator section of the (ARS).

The mass Flowrate passes through the (AH) is (m_s) in any case, where it comes directly from the storage tank [fig. (6a)] or a mixing from the storage tank with a fraction [f_2] coming from (ARS) through the 3 – way valve (V_2) [fig. (6b)] when [T_{st}] becomes larger than [T_{ref}], the 3 – way valve (V_2) is opened by a control panel signal.

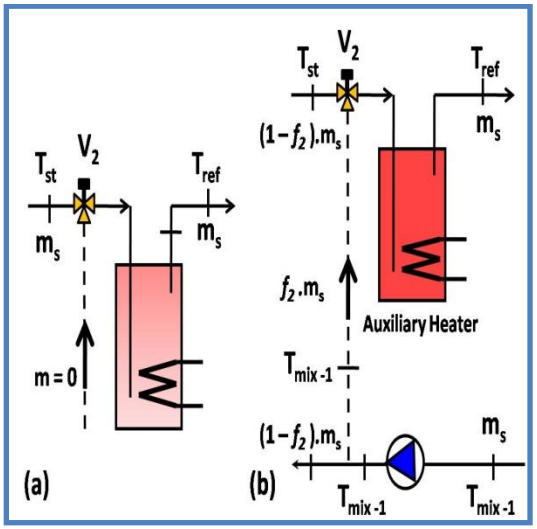

Figure (6): Schematic diagram of the Auxiliary Heater & 3 – way valve (V_2).

Or, it will be fully opened when (T_s) becomes less than (T_{mix-1}). So,

$$f_2 = \begin{cases} 0 & \text{when} \quad T_{st} < T_{ref} \\ > 0 \ \& \ < 1 & \text{when} \quad T_{st} > T_{ref} \\ 1 & \text{when} \quad T_{st} < T_{mix-1} \end{cases}$$

Thus, for [$f_2 = 0$], the heat added by the (AH) [fig. (6a)] will equal to:

$$Q_{AH} = m_s . C_{pw} . (T_{ref} - T_{st}) \quad \ldots\ldots (14)$$

And, for [$f_2 > 0$], there is no heat added by the (AH) [fig. (6b)], but the mass flow rate and the temperature become:

$$m_s = f_2 . m_s + (1 - f_2) . m_s$$

$$T_{ref} = f_2 . T_{mix-1} + (1 - f_2) . T_{st} \quad \ldots\ldots (15)$$

The General equation for the storage tank temperature (T_{st}):

By neglecting the effect of the pump power on the feeding temperature (T_{ci-n}) to the solar collectors, it means that ($T_{ci-1} = T_{st} + \Delta T$), then substituting (T_{co-n}) from eq. (9), and (T_{mix-1}) from eq. (13) for partial load into eq. (10), we will obtain:

$$\frac{dT_{st}}{dt} + K_6 . T_{st} = K_4 . [K_1 . (T_{st} + \Delta T) + K_2 . I_t + K_3 . T_a] + K_5 . [f_1 . T_{ref} + (1 - f_1) . T_G] - K_4 . \Delta T$$

Re-arranging the above equation, we find that:

$$\frac{dT_{st}}{dt} + K_7 . T_{st} = K_8 . I_t + K_9 . T_a + K_{10} . \Delta T + K_5 . [f_1 . T_{ref} + (1 - f_1) . T_G] \quad \ldots\ldots (16)$$

Where:

$$K_7 = (K_6 - K_1 . K_4), \quad K_8 = K_2 . K_4, \quad K_9 = K_3 . K_4, \quad K_{10} = K_4 . (K_1 - 1)$$

The Solar Radiation Intensity (I_t):

Equation (16) is a Non – Homogenous Linear differential equation of first order with constant coefficients, the non – homogeneity is due to presence of the dependant variable (I_t) the global solar radiation which is a function of time (t), the ambient temp.(T_a) in which it will be taken as the average daily day temperature (from the sunrise time to sunset time), the driving force temperature difference (ΔT) is also supposed as a fixed value, (T_{ref}) is specified as a minimum allowable

temperature into the generator section of (ARS), and (T_G) is maintained constant, because lowering (T_G) causes a lower in condensing temperature of (ARS) to un-achieved condensing temperature and to LiBr crystallization [ref. 24]. All those parameters can be considered as constants. So, to solve equation (16), the relation as a function [$I_t = f(t)$] should be known.

The simple Half – Sine Model of clear – day solar radiation is all that needed to predict the solar energy system design [ref. 9]. The only input required is the times of sunrise, sunset and the peak noontime solar irradiance, the model state that:

$$I_t = I_{noon}.\sin\left[\frac{\pi.\ (t - t_{sunrise})}{(t_{sunset} - t_{sunrise})}\right]$$

Letting the sunrise time ($t_{sunrise}$) to be the zero time, then ($\Delta t = t_{sunset} - t_{sunrise}$) represents the daylight time and the above equation for (I_t) becomes:

$$I_t = I_{noon}.\ \sin\left[\frac{\pi.\ t}{\Delta t}\right] \quad \ldots\ldots(17)$$

Substituting eq. (17) into eq. (16), we will obtain:

$$\frac{dT_{st}}{dt} + K_7\,.\,T_{st} = K_8\,.\,I_{noon}.\ \sin\left[\frac{\pi.\ t}{\Delta t}\right] + K_{11} \quad \ldots\ldots(18)$$

Where:

$$K_{11} = K_9\,.\,T_a + K_{10}.\ \Delta T + K_5.[\,f_1.T_{ref} + (1 - f_1).T_G]$$

Equation (18) has two solutions, the Complementary function and the Particular Integral [15], the complementary function can be find by equating the left side of eq. (18) to zero:

$$\frac{dT_{st}}{dt} + K_7\,.\,T_{st} = 0$$

It is natural to find out that the complete solution of homogenous equation mentioned above is:

$$T_{st-c} = C.\,e^{-K_7.\ t}$$

It easy to see that the Particular Integral solution is [ref. 15]:

$$Y_P = E + A.\sin\left[\frac{\pi.\ t}{\Delta t}\right] + B.\cos\left[\frac{\pi.\ t}{\Delta t}\right]$$

Differentiating (Y_P), and substituting for (Y_p & Y_p') into eq. (18) and solving for the constants (E, A & B), it is found that:

$$E = \frac{K_{11}}{K_7}, \qquad A = \frac{K_8.\ K_7.\ I_{noon}}{(K_7^2 + K_{12}^2)}, \qquad B = -\frac{K_8.\ K_{12}.\ I_{noon}}{(K_7^2 + K_{12}^2)}$$

Where:

$$K_{12} = \frac{\pi}{\Delta t}$$

Then the general solution for equation (18) is:

$$T_{st} = C.\,e^{-K_7.\ t} + \frac{K_{11}}{K_7} + \frac{K_8.\ I_{noon}}{(K_7^2 + K_{12}^2)}.\left[K_7.\ \sin\left[\frac{\pi.\ t}{\Delta t}\right] - K_{12}.\ \cos\left[\frac{\pi.\ t}{\Delta t}\right]\right] \quad \ldots\ldots(19)$$

The arbitrary constant (C) can be obtained by applying the initial condition at the beginning of the heating process by the Solar Energy which is:

$$\text{at } t = 0 \Longrightarrow T_{st} = T_i$$

Where (T_i) is the initial storage tank temperature. Substituting in equation (19) the general equation and solving for (C), which yields to:

$$C = T_i - \frac{K_{11}}{K_7} + \frac{K_8 . K_{12} . I_{noon}}{(K_7^2 + K_{12}^2)}$$

Rearranging the general solution to have the final form for (T_{st}) which becomes:

$$T_{st} = T_i . e^{-K_7 . t} + C_1 . (1 - e^{-K_7 . t}) + I_{noon} . \left\{ C_2 . \left(e^{-K_7 . t} - \cos\left[\frac{\pi . t}{\Delta t}\right] \right) + C_3 . \sin\left[\frac{\pi . t}{\Delta t}\right] \right\} \quad \ldots\ldots (20)$$

Where:

$$C_1 = \frac{K_{11}}{K_7} ; \qquad C_2 = \frac{K_8 . K_{12}}{K_7^2 + K_{12}^2} ; \qquad C_3 = \frac{K_8 . K_7}{K_7^2 + K_{12}^2}$$

The performance of the solar system is characterized by the solar fraction (SF), which is the fraction of load covered by the solar system given by the following equation [ref. 2]:

$$\text{Solar fraction (SF)} = \frac{Q_{load} - Q_{aux}}{Q_{load}} \quad \ldots\ldots (21)$$

The Application:

In this paragraph, a modeling design for Absorption Refrigeration system – single stage (effect) of [10.5 kW] capacity will be put into practice. This capacity represents the refrigeration effect [cooling output (Q_E)], the COP is an index of the efficiency of (ARS), it is calculated by dividing the cooling output (Q_E) by the required heat input (Q_G) [ref. 17] {see fig. (1) above}:

$$COP = \frac{Q_E}{Q_G + W_{me}} \approx \frac{Q_E}{Q_G}$$

Where (W_{me}) is the pump power which is small compared to (Q_G). Since COP for single – stage (ARS) is between (0.6 – 0.8) [ref. 6 & 18], and has a value of (0.7) [ref. 19], thus:

$$Q_G = \frac{10.5}{0.7} = 15 \text{ kW}$$

The (15 kW) is the required heat to be supplied by the solar heating system into the generator section, and from this point the other design factors will be found or proposed.

To find the total collectors area (A_c) required to produce the designed thermal load (Q_G), it will be estimated according to the following equation which will be used [ref. 5 & 20]:

$$A_{c-T} = \left(\frac{Q_G}{\eta . I}\right) . (\% \text{ Solar Availability })$$

To find the Average monthly Solar Insolation (I), we will consider summer months [April to September], and from the Meteorology Database for Baghdad City (year 2000) [ref. 26], we found that (I = 565 W/m^2), figure (7) shows the monthly variation in Solar Insolation of summer months.

For the efficiency □□□, it can be found in manufacturer's specification sheets or from the Solar Rating and Certification Corporation (SRCC), we will use an efficiency value of (0.45) which is an average of all the efficiencies of the brands [ref. 20]. The %Solar Availability is assumed to be equal to (100%) for unobstructed solar window. Thus the total collectors' area (A_{c-T}) can be obtained to be equal to:

A_{c-T} = 15000 / (0.45 * 565) = 59 m^2

To find the Collector's numbers to be used in this calculation, we should choose the standard area of the collector, this parameter is the manufacturer's specification and should be taken from collector's brochures, it is mostly equal to (2.87 m^2) for (8 ft x 4 ft) standard, and thus the collector's no. is:

Collector's no. (N) = 59 / 2.87 ≈ 20

These collectors {Glazed Flat – Plates [with double anti-reflection glazing and hermetically sealed collectors with inert – gas filling reduce collector heat losses, and can be used for applications in the range of (80 – 120 ℃)]} [ref. 3 & 21] or (Evacuated Tube) will be flushed mounted horizontally on the Building roof in parallel and series array, so it should be taken into consideration the enough space for this arrangement.

The Storage Tank capacity (size) depends on the system used, it can The collector's mass flow rate (m_{co-T}), it will be considered water instead of glycol, the optimum fluid flow rates per unit collector's area are usually in the range of (0.0083 to 0.0167 kg/s . m^2) [ref. 22] or (0.011 to 0.0146 kg/s . m^2) [ref. 23], we will use here for our calculated area (0.011 kg/s.m^2) to have total flow rate of (0.6 kg/s), that means the flow rate per one collector is equal to:

$$m_{co} = \frac{m_{co-T}}{\text{no. of collector (N)}} = \frac{0.6}{20} = 0.03 \text{ kg/s}$$

The solar collectors will be arranged in an array of two row in parallel, which means that no. of row (n = 2). So, the flow rate for two rows in series becomes equal to:

$$m_{co-2} = 2 * 0.03 = 0.06 \text{ kg/s}$$

roughly estimate to be equal to (0.05 to 0.075 m^3 / m^2 of the collectors' area) [ref. 12 & 22], thus it will be assumed to be (4.5 m^3 or 4500 Liter). Most Glazed Flat plate collectors are provided with values of (F_R (□□) = 0.68 to 0.75) & (F_R U_L = 4.9 to 5.247 W/m^2. ^oC) [ref. 11 & 13], choosing (F_R (□□) = 0.74) & (F_R U_L = 5.247 W/m^2 . ^oC) to be used in our calculation.

The average daylight ambient temperature (T_a) for 21st of each month can be obtained from Meteorology Database (2000) for Baghdad City [ref. 26] according to the following table (1):

The peak noontime Solar radiation [I_{noon} (W / m^2)] for 21st of each month can also be obtained from Meteorology Database (2000) for Baghdad City as shown in the following table (2) and fig. (8) shows the estimated values for it according to equation (17) for some months.

(ΔT) the driving force temperature differences is taken to be (5 ^oC) and the Initial Storage Water Tank (T_i) to be equal to ambient temp. (T_a) of the initiation working day.

In order to maintain good heat transfer in the generator section, only a small temperature difference [$\Delta T_G = T_{ref} - T_G$] can be tolerated in the hot water flow stream [ref. 19].

This is a result of the fact that the (ARS) was originally designed for steam input to the generator, and the heat transfer from the condensing steam is a constant temperature process. A temperature difference of (ΔT_G = 4 ℃) [ref. 24], and (ΔT_G = 7.5 ℃) [ref. 25], we will use a temperature difference of (ΔT_G = 6 ℃), i.e., if (T_{ref} = 95 ℃), then (T_G = 89 ℃).

According the above paragraph, the flow rate passing through the generator section ($\boldsymbol{m_s}$) can be estimated using Thus, for April month as an example, the constants ($K_1 - K_{12}$) can be estimated to have the following values, and equation (20) for April month becomes:

$K_1 = 0.884$, $K_2 = 0.0164$, $K_3 = 0.116$, $K_4 = 0.408$, $K_5 = 0.48$, $K_6 = 0.89$, $K_7 = 0.527$, $K_8 = 0.007$, $K_9 = 0.047$, $K_{10} = -0.047$, $K_{11} = 43.95$, $K_{12} = 0.224$,

$$C_1 = \left[\frac{43.95 + 2.88\, f_1}{0.527}\right],\quad C_2 = 0.005,\quad C_3 = 0.011$$

$$T_{st} = 31\, e^{-0.527\, t} + \left[\frac{43.95 + 2.88\, f_1}{0.527}\right] * (1 - e^{-0.527\, t}) + \{3.6\,(e^{-0.527\, t} - \cos[0.224\, t]) + 7.92\, \sin[0.224\, t]\}$$

Results and discussion

The analysis for this research shows the possibility to predict the Storage Tank Water temperature (T_{st}) for the solar absorption refrigeration system and the factors that have major effects on system operation during any day in the year and the succession.

Figure (9a) shows the variation of Storage Tank temperature (T_{st}) variation during the heating time for 21st of April starts at sunrise time (5 O'clock a.m.) and ends at sunset (7 O'clock p. m) according to the above equations for solar collector arranged in two series rows (2 x 10 = 20).

Figure (9b) shows also (T_{st}) variation during the heating time for 21st of April but for solar collector arranged in one row (1 x 20 = 20). The results showed that there wasn't a significant difference in (T_{st}) between the two arrangements as tabulated in table (3):

equation (11), to yield that (m_s = 0.6 kg/sec).

The reason for this point can be explained through the change in values of the constants (K_1, K_2 and K_3) of equation (9) which are shown in fig. (10). It can be observed that the value of (K_1) is increased with increasing number of rows, on contrary the values of (K_2 and K_3) is decreased with increasing number of rows, that means the increasing in (K_1) is compensated by the decreasing in values of (K_2 and K_3), thus the outlet temperature from the solar collectors (T_{co-n}) is considerably unchanged.

Actually, the initial storage tank temperature in a continuous operation will be the generator outlet temperature (T_G) of (ARS) not (T_i). So, on this basis the storage tank temperature will become as shown in the following figures.

It is obviously seen from fig. (11) that the storage tank temperature for 21st of July (with noon solar intensity of 780 W/m^2) is lowered first to below than (89 ^{o}C) then it goes up again to reach and pass (89 ^{o}C), this is because the solar collectors has its own thermal capacity to rise from its initial temperature to reach the temperature of (89 ^{o}C), and the solar radiation intensity should reach the critical solar intensity (I_c) which is equal [ref. 3]:

$$I_c = U_L.\frac{(T_{ci} - T_a)}{(\tau\alpha)}$$

For example the critical solar intensity for September month can be computed to be equal to (490 W/m^2), which occurs at about approximately at (10 a.m.)

The same thing is shown in fig. (12) for the storage tank temperature for 21st of September (with noon solar intensity of 630 W/m^2), but the difference is the time

required to reach and pass the (89 ^{o}C) is less and with higher (T_{st}) for higher solar intensity rather than a lower solar intensity, which is apparently clear in figures (11 & 12) that the useful time for effective solar intensity is between (9 a.m. to about 6 p.m.) for July and (10 a.m. to 5 p.m.) for September.

The effect of the storage tank capacity was studied in this research to obtain the best size or tank capacity that the solar heating system has for (ARS). Different tank capacity is used in our computation and the final results were collected in figure (13).

It is observed that for small storage capacity (1500 kg), the storage tank temperature drops rapidly in a short time to its minimum temperature and then rise to pass the line of (89 ^{o}C) because it has a lower thermal capacity which means it lost its heat quickly. On contrary, for larger storage tank (4500 kg), the storage temperature drops slowly (due to its high thermal capacity) to its minimum temperature which is higher than the minimum temperature for storage tank of (1500 kg) but with a time lags and then rise to pass the line of (89 ^{o}C).

It appears also from fig. (13) that the storage tank temperature for lower storage tank capacity speeds up to its maximum temperature and then drops rapidly, it is also due to its lower thermal capacity, whereas the storage tank temperature for larger tank capacity rises slower to its maximum temperature which is lower than that for smaller tank but with a time lags to last for a wider period of time than smaller tanks.

The effect of the storage tank capacity on the collector's outlet temperature is well explained in fig. (14)., the figure shows no significant impact on the collector's outlet temperature for different storage tank capacity (4500, 3000 & 1500 kg), and the three curves for them seem to be coincided on each other, the best is (4500 kg) storage tank as expressed in the previous paragraph.

In figure (15), the collector's outlet temperature is drawn against the collector's inlet temperature. The figure shows that at beginning the solar collectors start to absorb the heat from the circulated flowrate through them to reach its equilibrium thermal state due to two reasons:

- The initial collector's temperature is nearly equal to the ambient temperature, so it starts to absorb the heat from the circulating flow rate through them.
- The solar intensity doesn't reach to its critical intensity to compensate the heat losses from the collectors themselves until it reaches the balance points which is marked with the bold line in fig. (15), and same thing happen when solar intensity drops to (I_c) at sun's setting.

The auxiliary heat added by the (AH) is computed and explained in fig. (16).

The figure shows that the auxiliary heat added is high because the storage tank temperature at its initiation is lowered as the storage tank gives some of its thermal capacity to warm up the solar collector till the solar intensity reaches its critical value. Thus a bypass 3 – way valve (V_2) is incorporated and comes into play to pass the flow rate at a generator outlet temperature (T_G) directly to the auxiliary heater (AH) till the storage tank temperature rise up to be equal to the generator outlet temperature (T_G) and again to be full opened the 3 – way valve when the storage tank temperature drops again lower than the generator outlet temperature.

❖ The solar fraction which is a feature of the solar system performance is also computed and explained in fig. (17) below. It shows that solar fraction increases as the load decreases and the useful time for solar contribution becomes wider for lower partial loads.

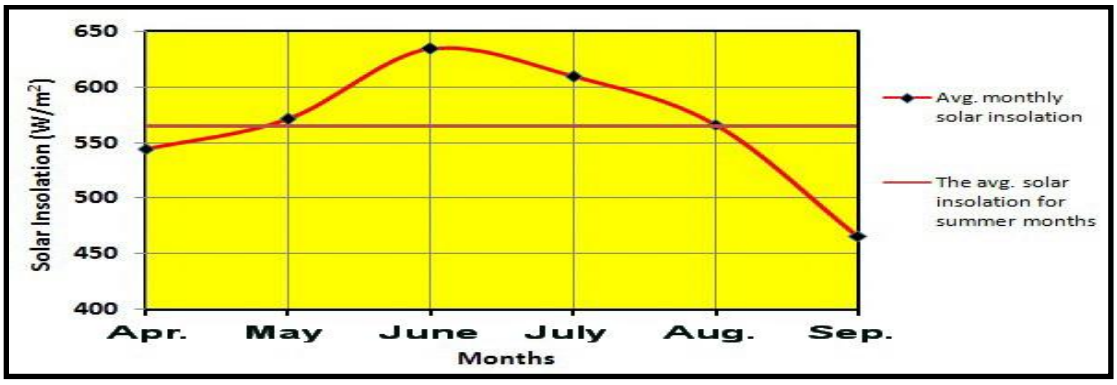

Figure (7): The monthly Avg. solar insolation and the Avg. of summer months.

Table (1): The Avg. daylight ambient temp. for 21st of each month [ref. 26].

Month	Jan.	Feb.	Mar.	Apr.	May	June	July	Aug.	Sep.	Oct.	Nov.	Dec.
(T_a) Avg. daylight ambient temp. (^oC)	11.83	15.00	23.73	31.00	32.30	34.40	41.56	39.36	31.30	27.60	16.72	13.15

Table (2): The Peak Noon Solar Radiation for 21st of each month [ref. 26].

Month	Jan.	Feb.	Mar.	Apr.	May	June	July	Aug.	Sep.	Oct.	Nov.	Dec.
($t_{sunset} - t_{sunrise}$) Δt (hour)	10	10	12	14	14	14	14	14	14	12	10	10
I_{noon} Peak noon Solar Radiation (W/m^2)	493	595	675	720	760	732	780	722	629	594	455	408

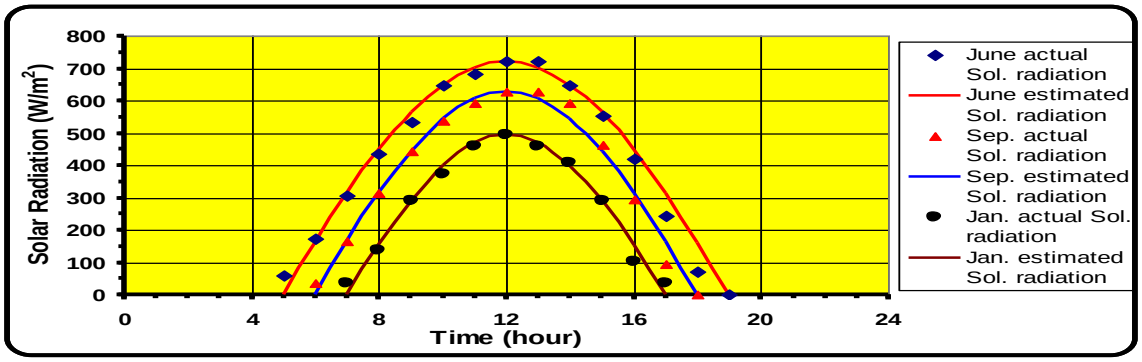

Fig. (8): The Estimated and Actual Sol. Radiation for 21st of some months.

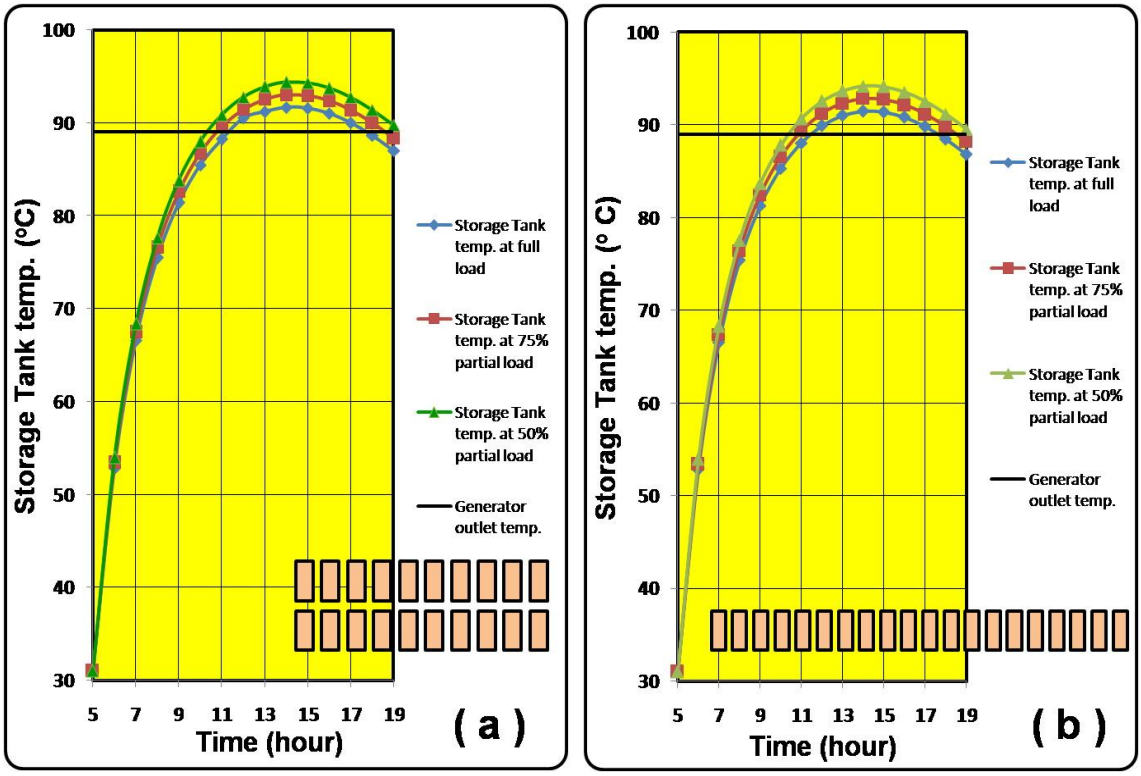

Fig. (9): (a) Storage tank temp. for solar collectors arranged in two series row. (b) Storage tank temp. for solar collectors arranged in one row.

Time	1 row (with partial load)			2 row (with partial load)		
	100%	75%	50%	100%	75%	50%
5	31	31	31	31.00	31.00	31.00
6	52.81	53.37	53.93	52.84	53.40	53.96
7	66.50	67.39	68.28	66.57	67.46	68.35
8	75.36	76.44	77.52	75.47	76.55	77.64
9	81.26	82.46	83.65	81.40	82.60	83.80
10	85.29	86.55	87.82	85.46	86.73	87.99

11	88.05	89.36	90.66	88.24	89.55	90.85
12	89.89	91.22	92.54	90.51	91.42	92.75
13	90.99	92.33	93.67	91.19	92.54	93.89
14	91.46	92.81	94.16	91.67	93.02	94.38
15	91.38	92.73	94.08	91.59	92.95	94.31
16	90.80	92.16	93.52	91.02	92.38	93.74
17	89.80	91.16	92.51	90.02	91.38	92.74
18	88.43	89.79	91.15	88.65	90.02	91.38
19	86.79	88.15	89.51	87.01	88.38	89.74

Table (3): Storage tank temp. for 21st of Apr. for 1 row & 2 row arrangement.

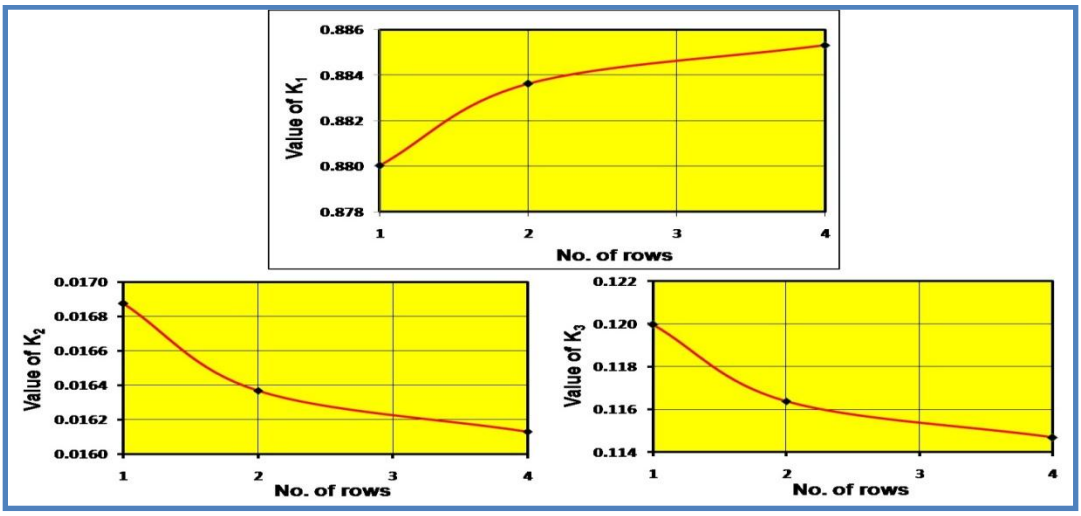

Fig. (10): The change of the constants values (K_1, K_2 & K_3) with no. of collector's rows.

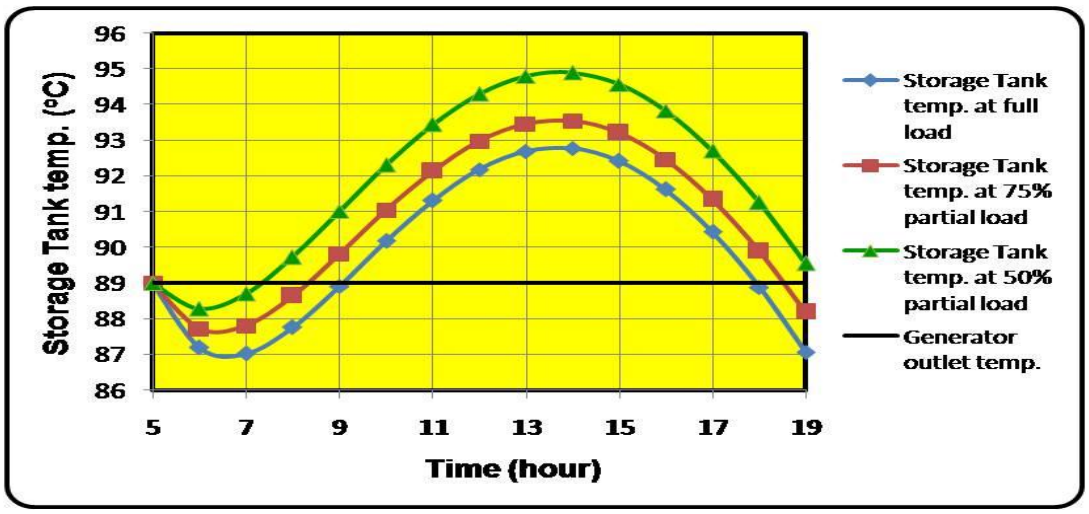

Fig. (11): Storage tank temp. for 21st of July at different loads.

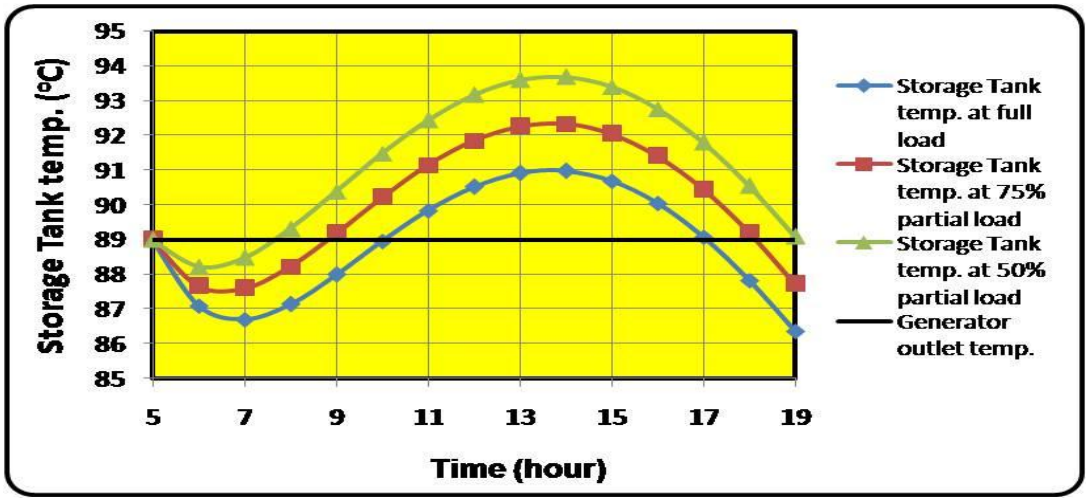

Fig. (12): Storage tank temp. for 21st of September at different loads.

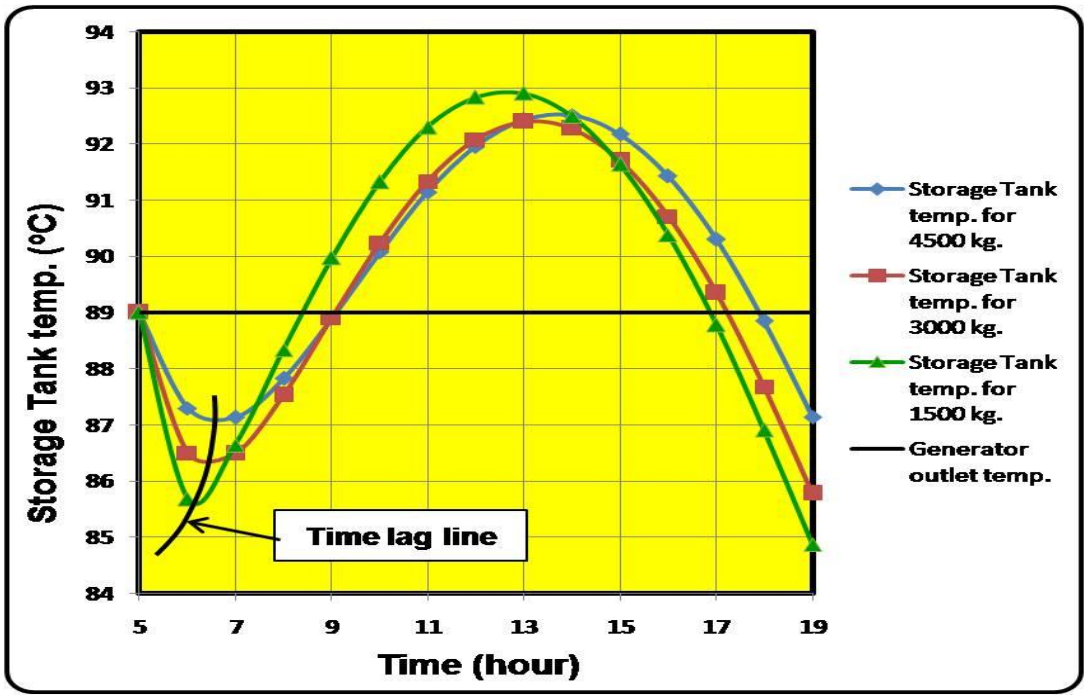

Fig. (13): Storage tank temp. for 21st of June for different storage tank capaciies.

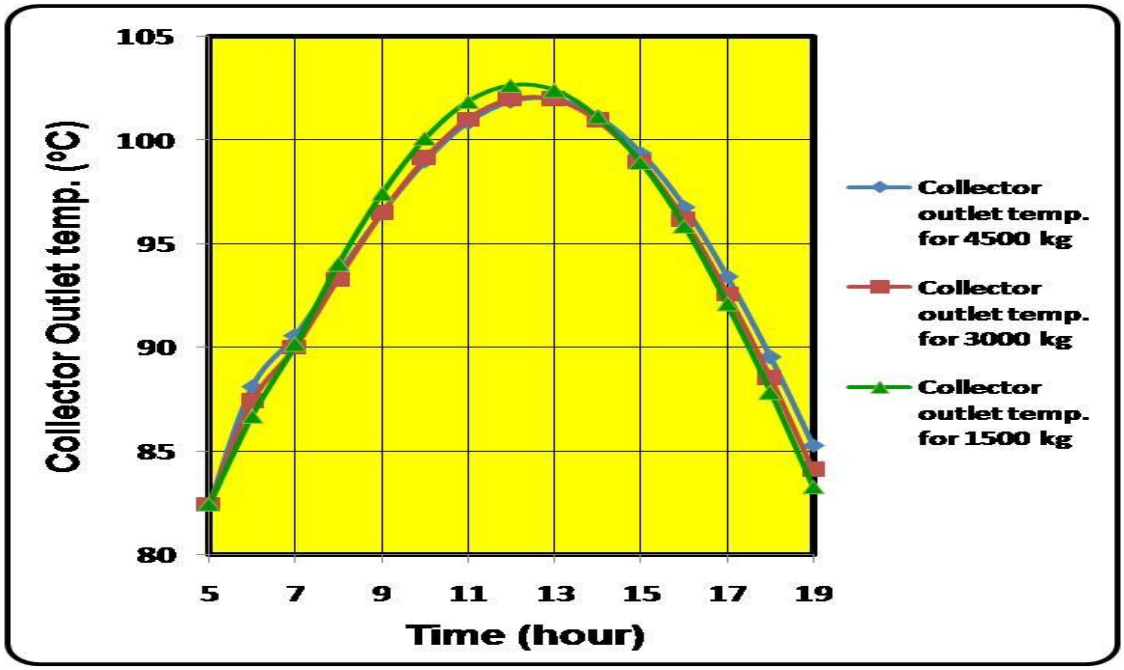

Fig. (14): Collector's outlet temp. for 21st of June for different storage tank capacities.

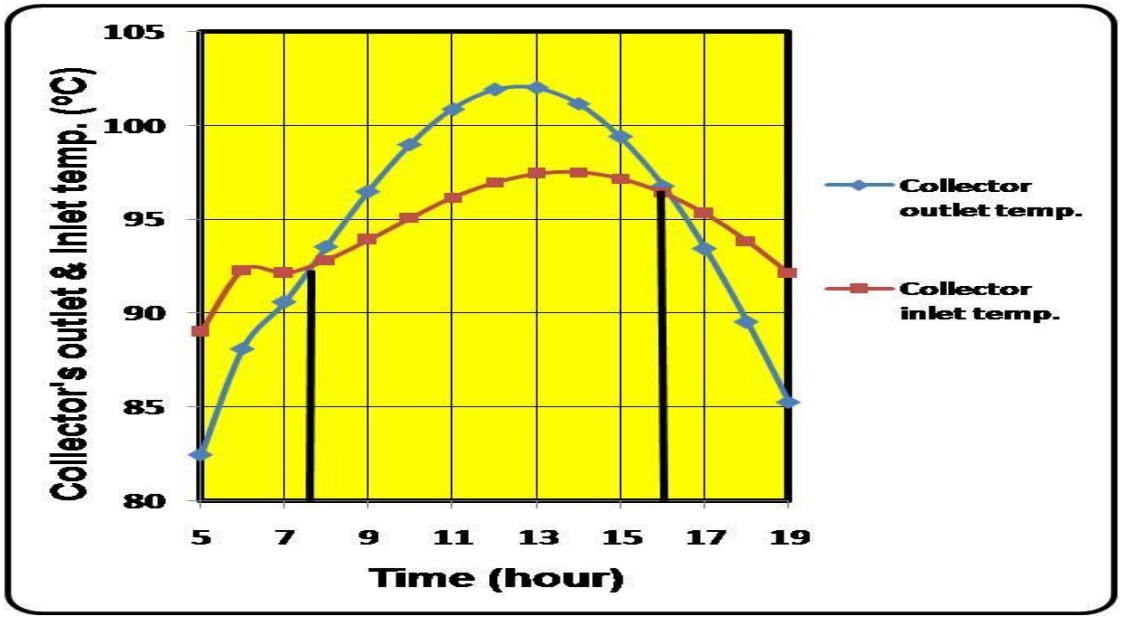

Fig. (15): Collector's outlet and inlet temp. for 21st of June for (4500 kg) storage tank capacity.

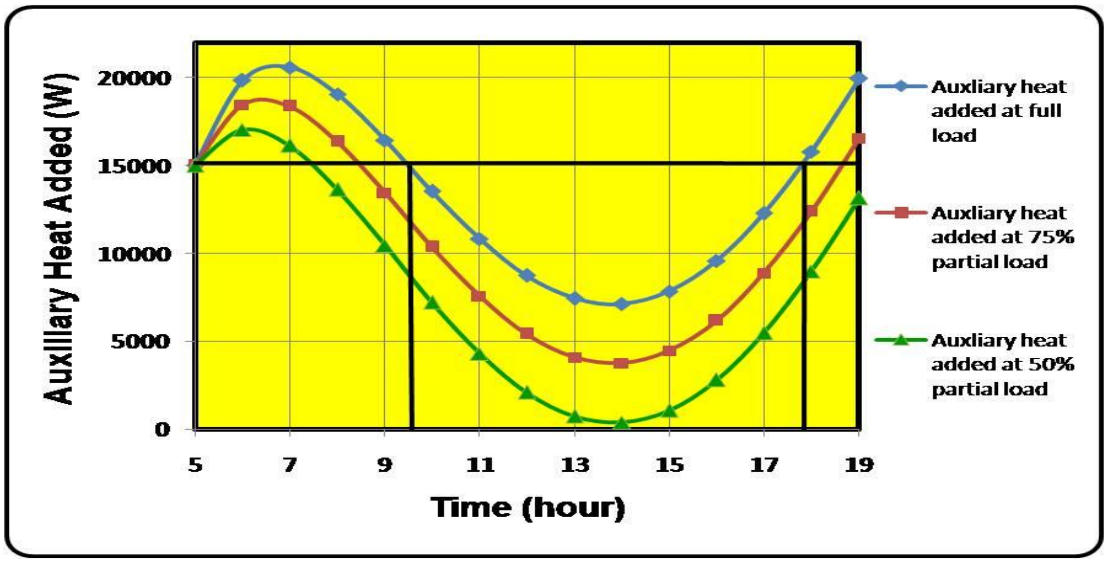

Fig. (16): The auxiliary heat added for 21st of June at different loads.

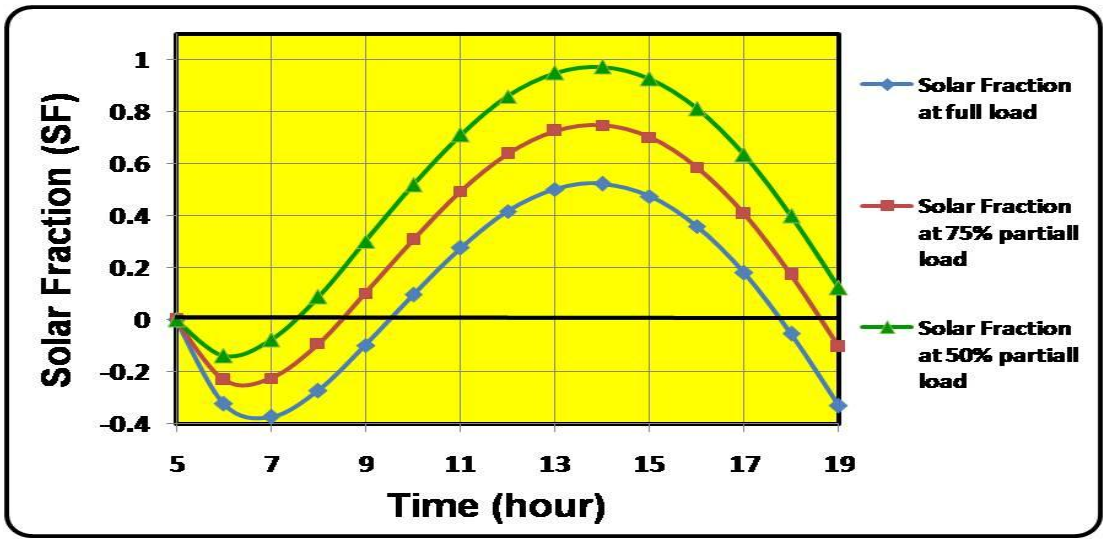

Fig. (17): The solar fraction variation for 21st of April at different loads.

Conclusion

The following conclusions were attained from the foregoing model and design:

- The collector's outlet temperature wasn't influenced with collectors arrangement arrays [to be in one parallel array (1 x 20) or in two row in series arrangement array (2 x 10) or more], the variation is not more than (0.7%) as shown in table (3) and (fig. 9), this is because the received solar energy is the same for the same number

of collectors, unless the flow rate of one collector is passed through the collectors in series, in this case only, the collector's outlet temperature will be raised to a higher temperature. In other words for same thermal load to reach high temperature, the number of collectors should be increased.

- Referring to (fig. 13), using different storage tank capacity (size), the best is larger tank because it is found that there is no significant rise in collector's outlet temperature, when using smaller tank size the maximum temperature is about (T_{st} = 92.9℃) whereas for larger tank (T_{st} = 92.6℃), but there is a wider period of useful solar time when using larger tank, it starts from 9:00 o'clock to end at about 18:00 o'clock (It is an economical point of view).
- Referring to (fig. 11), at partial load, it is found that the maximum storage tank temperature is increased from (T_{st} = 92.8℃) at full load to (T_{st} = 94.9℃) at 50% partial load and a wider period of useful solar time are increased from (9:00 o'clock to 18:00 o'clock) at full load to (7:30 o'clock to about 19:15 o'clock) at 50% partial load.
- Referring to (fig. 17), the maximum solar fraction (*SF*) is also increased from about (0.5) at full load to about (0.95) at 50% partial load. Working with partial load looks like increasing number of solar collectors.

References

[1] Yuting WU, Jianxun REN, Zengyuan GUO, Chongfang MA, "Dynamic Simulation of Closed Brayton Cycle Solar Thermal Power System", International Conference on Sustainable Energy Technology. Nottingham, UK, (28 – 30) June 2004.

[2] Sophie V. Masson, Minh Qu, David H. Archer, "Performance Modeling of a Solar Driven Absorption cooling system for Carnegie Mellon University Intelligent Workplace".

[3] Frank Kreith,D. Yogi Goswami, "Handbook of Energy Efficiency & Renewable Energy", ch. 20, 2007, Taylor & Francis Group, LLC., USA.

[4] V Mittal, KS Kasana, NS Thakur, "The Study of Solar Absorption Air Conditioning Systems", Journal of Energy in Southern Africa. Vol. 16 No. 4, Nov. 2005.

[5] V Mittal, KS Kasana, NS Thakur, "Modeling and Simulation of a Solar Absorption Cooling Systems for India", Journal of Energy in Southern Africa. Vol. 17 No. 3, Aug. 2006.

[6] Soteris A. Kalogirou, "Solar Thermal Collectors & Applications", Progress in Energy & Combustion Science, 30 (2004). www.sciencedirect.com.

[7] Zdzisław Pakowski and Arun S. Mujumdar, "Handbook of Industrial Drying", ch. 3. 3rd ed. 2006 by Taylor & Francis Group, LLC.

[8] Soteris A. Kalogirou, "Solar Energy Engineering – Processes & Systems", 1st ed., 2009, Elsevier Inc., USA.

[9] William B. Stine & Michael Gayer, "Power From The Sun ", 2001, chapter 5.

www.PowerFromTheSun.net.

[10] Lunde, P. J., "Solar Thermal Engineering", John Wiley & Sons, New York. (1980).

[11] Solar Water Heating Project Analysis (RETScreen Engineering & Cases Textbook)

www.retscreen.net.

[12] Duffie, J. A., "Solar Energy Thermal Process". A Wiley Interscience Publication, (1974).

[13] Thomas, B, & supervisor Dr. Naoko Ellis." Solar Thermal Water Heating (A simplified Modelling Approach & Potential Application for CHBE)",

www.chbe.ubc.ca/sustainability/docs/CHBE492_SolarThermal.pdf.

[14] EE IIT, Kharagpur,"Lesson – 15, Absorption Refrigeration System – based on water / LiBr pair", 2008, India.

http://nptel.iitm.ac.in/courses/Webcourse-contents/IIT-Kharagpur/

[15] Attenborough M., "Mathematics for Electrical Engineering & Computing", Newness, (2003) (An imprint of Elsevier), Oxford.

[16] Jasim M. Abdulateef, Kamaruzzaman Sopian, M. A. Alghoul, Mohd Yusof Sulaiman, Azami Zaharim & Ibrahim Ahmed,"Solar Absorption Refrigeration System Using New Working Fluid Pairs", International Journal of Energy, Issue 3, Vol. 1, 2007.

[17] EE IIT, Kharagpur,"Lesson – 14, Absorption Refrigeration System – based on water / LiBr pair", 2008, India.

[18] Duffie J. A. and Beckman W. A.,"Solar Engineering of Thermal Process", Wiley, N.Y, 1991.

[19] Kevin D. Rafferty, P.E."Chapter 13 – Absorption Refrigeration",

http://geoheat.oit.edu/pdf/tp51.pdf

[20] Sorter, A., Miess, K., Engel, R. & Sorensen, A. Solar Thermal Design: Research, Design and Installation of Solar Water System for Redwood National Park.

www.ajur.uni.edu/v1no4/Sorter et al.pdf

[21] Björn Nienborg, "Solar-assisted heating and cooling of buildings: technology, markets and perspectives", http://www.solarserver.de/solarmagazin/index-e.html

[22] Ursula Eicker, "Solar Technologies for Buildings", John Wiley & Sons Ltd, USA, 2003.

[23] J. Paul Guyer, , "Introduction to Solar Cooling Systems",

http://www.cedengineering.com/upload/Intro%20To%20Solar%20Cooling%20Systems.pdf

[24] Soteris Kalogirou, George Florides, Savvas Tassou, Louis Wrobel**,"** Design and Construction of a Lithium Bromide Water Absorption Refrigerator", *CLIMA 2000/Napoli 2001 World Congress – Napoli (I), 15-18 September 2001*

http://ktisis.cut.ac.cy/bitstream/10488/881/1/C43-CLIMA-LITHIUM.pdf

[25] R. Palacios Bereche, R. Gonzales Palomino, S. A. Nebra," Thermoeconomic Analysis of a Single and Double-Effect LiBr/H2O Absorption

Refrigeration System", Int. J. of Thermodynamics, Vol. 12 (No. 2), pp. 89-96, June 2009.

[26] Meteorology Database for Baghdad City (1998).

تصميم نموذج لمنظومة تسخين شمسية تستخدم الطاقة الحرارية المتولدة فيها كقدرة حرارية دافعة لمنظومة تبريد امتصاصية

محمد هادي علي

الجامعة المستنصرية

الخلاصة:

إن هذا البحث يدرس تصميم نموذج لمنظومة تسخين شمسية تستخدم الطاقة الحرارية المتولدة فيها كقدرة حرارية دافعة لمنظومة تبريد إمتصاصية – ذات مرحلة واحدة يستخدم فيها محلول الليثيوم بروماید (LiBr solution), وهذه المنظومة تستخدم ألواح التجميع الشمسية المستوية (Flat – Plate Collector), حوض التخزين الحراري (The Thermal Storage Tank), السخان الإضافي (Auxiliary Heater) و الصمامات الثلاثية (3-way valves). ذهب البحث أيضا إلى دراسة الحمل الحراري الجزئي من خلال التحكم بكمية المائع المتدفق عبر وحدة التوليد (generator) لمنظومة التبريد الإمتصاصية, وأيضا دراسة تأثير ترتيب ألواح التجميع الشمسية على هيئة مصفوفات بالتوالي أو التوازي على كفاءة وأداء المنظومة الشمسية.

لقد تركزت الدراسة على تخمين وحساب أداء المنظومة الشمسية طوال فترة الصيف. وكذلك دراسة تأثير المتغيرات التصميمية المختلفة وحالات التشغيل على أداء المنظومةالشمسية.

في هذا البحث, تم التوصل إلى معادلة رياضية عامة لدرجة الحرارة الخارجة من ألواح التجميع الشمسية على شكل مصفوفات متوالية.

وقد أظهرت النتائج الحسابية ما يلي:

- ليس هناك إختلاف أو فرق واضح أو مهم في درجة حرارة حوض التسخين لكلا من الترتيب المتوازي أو المتوالي لألواح التسخين الشمسية.
- لا تتأثر كثيرا درجة الحرارة الخارجة من الألواح الشمسية بسعة حجم حوض التسخين.
- تزداد درجة حرارة حوض التسخين مع زيادة نسبة الحمل الحراري الجزئي أي كلما قل الحمل الحراري.